On the Computation of the Pure Neumann Problem in 2-dimensional Elasticity

M. Steigemann[1]. M. Fulland[2]

[1] *Department of Mathematics and Natural Sciences, University of Kassel, Germany*
[2] *Westfälisches Umwelt Zentrum, Universität Paderborn*

Abstract. The accurate computation of stress intensity factors (SIFs) plays a decisive role in the determination of crack paths. The calculation of SIFs with the help of singular weight functions leads to pure NEUMANN problem for anisotropic elasticity in a plane domain with a crack. Here a method is presented to overcome the specific numerical difficulties which arises while calculating these solutions with Finite Element methods. The accuracy and advantage of this method are shown by a numerical example, the calculation of SIFs of a compact tension specimen.

Key Words: two-dimensional elasticity, finite elements, Neumann problem, stress intensity factors, anisotropic solids, weight functions.

Mathematics Subject Classification (2010) 65N22, 65N30, 74G15, 75R10, 74S05

1. Introduction

For many problems in elasticity theory it is important to compute solutions of the pure NEUMANN problem

$$-\nabla \cdot \sigma(u) = f \ \text{ in } \ \Omega, \qquad \sigma^{(n)}(u) = g \ \text{ on } \ \partial\Omega$$

where $\Omega \subset \mathbb{R}^2$ is some open domain. In particular, if the domain has a crack, in fracture mechanics one is often interested in computing the stress intensity factors K_j. Stress intensity factors (SIFs) play an essential role while computing the path of the crack in the solid under an external load. The accuracy of the computed crack path depends highly on the SIFs. For isotropic solids, there are various methods to compute these factors, but up to now, it is not clear, if this all works for anisotropic ones. Nevertheless, for every homogeneous anisotropic solid, K_I and K_{II} can be computed very accurately by evaluating an integral over so-called weight functions ζ^j and the applied loads, namely

$$K_j = \int_\Omega \zeta^j \cdot f \, dx + \int_{\partial\Omega} \zeta^j \cdot g \, ds, \qquad j = 1, 2.$$

These weight functions, introduced by MAZ'YA and PLAMENEVSKY [MP77], are composed of singular eigenfunctions of the elasticity operator in the half-plane with a semi-infinite crack and some special solutions of the NEUMANN problem in Ω. Eigenfunctions of the elasticity operator are known analytically for isotropic homogeneous solids and can be computed with arbitrary precision for anisotropic ones. The solution of the NEUMANN problem depends on the domain and has to be computed numerically.

A solution of the pure NEUMANN problem is uniquely determined up to a rigid motion only and the GREEN's formula implies, that the data f and g must be orthogonal to such motions. The direct

In: International Journal of Fracture, Volume 146 (2007), Page 265-277

GALERKIN discretization leads to a linear system of equations with a stiffness matrix $\boldsymbol{A}$ with three-dimensional kernel and a right-hand side orthogonal to this kernel. Computing a finite element solution from this system brings several numerical difficulties.

First of all, the linear system cannot be solved by a standard solver like the Conjugate Gradient method. One has to modify the method or has to use an other approach like the Minimal Residual method.
Moreover, a discrete solution only exists, if the discrete right-hand side is orthogonal to the kernel of $\boldsymbol{A}$. While computing the discrete right-hand side using quadrature formulas and with finite precision, the orthogonality condition is not fulfilled precisely. The accuracy of the numerical solution and the stress intensity factors will highly depend on this precision, while using the Minimal Residual approach.

To avoid these difficulties, a widely used basic approach to fix the solution is to prescribe the value on at least two nodes. This eliminates the kernel of the stiffness matrix and one can apply a conventional solver. The linear system is solvable for all right-hand sides. From a mathematical point of view, the computed finite element solution is only a weak solution in the SOBOLEV space $H^1(\Omega)$ and it is not obvious that such a solution is continuous or exists at a single point. Besides this, the numerical solution will have a peak at these nodes and this can destroy the computation of SIFs.

We want to follow another idea to solve the NEUMANN problem, presented in [BL05] for the Laplace equation. There exists a unique solution of the NEUMANN problem, if we look for a solution in a subspace of $H^1(\Omega)$, complementary to the space of rigid motions. Such a subspace $H_{\mathcal{R}}$ was introduced in [BS02] and with a projection

$$\mathcal{P}:\ H^1(\Omega) \longrightarrow H_{\mathcal{R}}$$

an arbitrary solution of the NEUMANN problem can be fixed uniquely in this subspace. This also works in the discrete case. Using a discrete analogue to $\mathcal{P}$, the unique numerical solution in $H_{\mathcal{R}}$ can be found from any numerical solution of the NEUMANN problem. The discrete projection can also be used to improve the accuracy of the orthogonality conditions of the discrete data.

In this paper we will consider a bounded domain with a crack and our main interest is to compute the displacement field and the stress intensity factors K_I and K_{II} under an external load. First, we will construct a subspace $H_{\mathcal{R}}$, complementary to rigid motions and a projection $\mathcal{P}$ onto it. On $H_{\mathcal{R}}$ we recall the existence and uniqueness of a weak solution.
We will show, that the GALERKIN discretization leads to a linear system with a three-dimensional null-space, while using LAGRANGIAN bilinear finite elements. It turns out, that the continuous orthogonality conditions are equivalent to the discrete ones. We give a discrete analogue of the projection $\mathcal{P}$ to compute the finite element approximation of the unique solution in $H_{\mathcal{R}}$ and we will show the advantages of this projection method. For a Compact Tension specimen, well-known in fracture mechanics, we will present numerical results, containing the displacement field and stress intensity factors.

2. The NEUMANN problem

Let G be a domain in the plane $\mathbb{R}^2$ with compact closure $\overline{G}$ and Lipschitz boundary Γ, containing the origin. We consider the pure NEUMANN problem of 2-dimensional elasticity theory in the domain

$\Omega := G \setminus \Xi$, where $\Xi := \{x \in \overline{G} : x_1 \leq 0, x_2 = 0\}$ is a rectilinear edge cut:

$$\begin{aligned} \mathscr{L}(\nabla_x)u(x) &= -\nabla \cdot \sigma(u) = f(x), && x \in \Omega, \\ \mathscr{N}(\nabla_x)u(x) &= \sigma^{(n)}(u) = 0, && x \in \Xi^+ \cup \Xi^-, \\ \mathscr{N}(\nabla_x)u(x) &= \sigma^{(n)}(u) = p(x), && x \in \Gamma, \end{aligned} \tag{1}$$

$n = (n_1, n_2)^\top$ is the outward normal, $u = (u_1, u_2)^\top$ the displacement vector, $f = (f_1, f_2)^\top$ the vector of body forces and $p = (p_1, p_2)^\top$ denotes the vector of surface load. With Ξ^+ and Ξ^- we denote the upper and lower sides of the crack, considered to be tension-free, see Figure 1. To omit technical difficulties, we also assume, that Ω can be divided in two LIPSCHITZ domains $\Omega^- = \{x \in \Omega : x_2 < 0\}$ and $\Omega^+ = \{x \in \Omega : x_2 > 0\}$. The strain tensor in cartesian coordinates is given by

$$\varepsilon_{ij}(u; x) = \frac{1}{2}\left(\frac{\partial u_i}{\partial x_j} + \frac{\partial u_j}{\partial x_i}\right), \qquad i, j = 1, 2,$$

and by HOOKE's Law, for the stress tensor the relation holds

$$\sigma_{ij}(u; x) = \sum_{k,l=1}^{2} a_{ij}^{kl} \varepsilon_{kl}(u; x), \qquad i, j = 1, 2.$$

The real constants a_{ij}^{kl}, called elastic moduli, satisfy the following symmetry and positivity conditions

$$a_{ij}^{kl} = a_{ji}^{lk} = a_{li}^{jk}, \qquad \sum_{i,j,k,l=1}^{2} \zeta_{ij} a_{ij}^{kl} \zeta_{kl} \geq c_0 \sum_{i,j=1}^{2} |\zeta_{ij}|^2, \quad c_0 > 0$$

for any symmetric real 2×2 matrix ζ. In an anisotropic material there are 6 different elastic moduli, for an isotropic material holds

$$a_{11}^{11} = a_{22}^{22} = \lambda + 2\mu \qquad a_{22}^{11} = a_{11}^{22} = \lambda \qquad a_{12}^{12} = a_{21}^{21} = \mu \qquad a_{11}^{12} = a_{22}^{12} = 0$$

with the LAMÉ constants λ and μ.

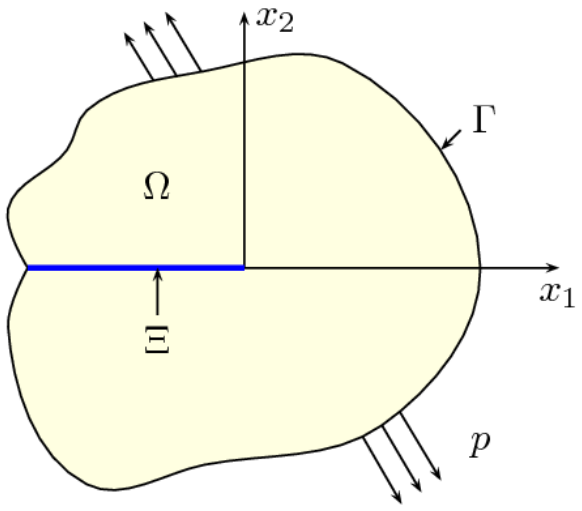

Figure 1: Homogeneous elastic body Ω with a rectilinear edge cut Ξ

3. The variational problem and weak solutions

We recall the definition of a weak solution. With $H^m(\Omega)$ we denote the usual SOBOLEV space of order m with norm

$$\|u; H^m(\Omega)\| = \left(\sum_{k=0}^{m} \|\nabla^k u; L^2(\Omega)\|^2 \right)^{1/2},$$

here we use the notation

$$\|\nabla^k u; L^2(\Omega)\|^2 := \sum_{|\alpha|=k} \|\partial_x^\alpha u; L^2(\Omega)\|^2.$$

The expression $(u,v)_\Omega := \int_\Omega u \cdot v \, dx$ indicates the inner-product of the LEBESGUE space $L^2(\Omega)$ and $H^{1/2}(\partial\Omega)$ denotes the space of traces equipped with the norm

$$\|u; H^{1/2}(\partial\Omega)\| := \inf \big\{ \|v; H^1(\Omega)\| : v \in H^1(\Omega) \text{ and } u = v \text{ on } \partial\Omega \big\}.$$

In our notation, we do not distinguish between scalar and vector-valued functions. The vector space of rigid motions is

$$\mathcal{R} = \big\{ u \in C^\infty(\mathbb{R}^2) : u = a + b \cdot x_{\mathcal{R}}, a \in \mathbb{R}^2, b \in \mathbb{R} \big\}$$

with $v_{\mathcal{R}}(x) := (v_2(x), -v_1(x))^\top$ for every field v. On the Lipschitz domain G for fields $u \in H^2(G)$, $v \in H^1(G)$ we have GREEN's formula

$$(\mathscr{L}u, v)_G + (\mathscr{N}u, v)_{\partial G} = a(u,v) \quad \text{with} \quad a(u,v) = \int_G \sum_{i,j=1}^{2} \sum_{k,l=1}^{2} a_{ij}^{kl} \varepsilon_{kl}(u) \varepsilon_{ij}(v) \, dx.$$

Note that $\frac{1}{2}a(u,v)$ is the elastic energy. As considered, Ω can be divided in two LIPSCHITZ domains Ω^+ and Ω^- and applying GREEN's formula to each, we find

$$a(u,v)_\Omega = \quad a(u,v)_{\Omega^+} + a(u,v)_{\Omega^-} = (\mathscr{L}u, v)_\Omega + (\mathscr{N}u, v)_{\partial\Omega} + (\mathscr{N}u, v)_{\gamma^+} + (\mathscr{N}u, v)_{\gamma^-}$$

with $\gamma := \big\{ x \in \overline{G} : x_1 > 0, x_2 = 0 \big\}$. If $u \in H^2(\Omega)$, $v \in H^1(\Omega)$, the traces on γ^+ and γ^- coincide. Taking into account the direction of the outward normal on γ^+ and γ^-, we find the equation

$$(\mathscr{N}u, v)_{\gamma^+} = -(\mathscr{N}u, v)_{\gamma^-}$$

and GREEN's formula still holds on Ω. For right-hand sides $f \in L^2(\Omega)$, $g \in H^{1/2}(\partial\Omega)$ with $g = p$ on Γ and $g = 0$ on Ξ, we call $u \in H^1(\Omega)$ a weak solution of the NEUMANN problem, if the relation

$$a(u,v) = (f,v)_\Omega + (g,v)_{\partial\Omega} =: F(v) \tag{2}$$

holds for all $v \in H^1(\Omega)$.

Clearly, $\mathcal{R} \subset H^1(\Omega)$ and since $a(u,v) = 0$ for all $u \in H^1(\Omega)$ and $v \in \mathcal{R}$, the data f and g must fulfill the necessary condition

$$\int_\Omega f \cdot v \, dx + \int_{\partial\Omega} g \cdot v \, ds = 0 \quad \text{for all} \quad v \in \mathcal{R}, \tag{3}$$

such functions are called self-balanced. On the other hand, if $a(u,v) = 0$ for all $v \in H^1(\Omega)$, then $a(u,u) = 0$, hence $\varepsilon(u) = 0$, which implies $u \in \mathcal{R}$ and thus a weak solution is determined up to a rigid

motion only. A weak solution can always be fixed if we look for $u \in H_{\mathcal{R}}$, where $H_{\mathcal{R}}$ is a (topological and algebraical) complement of the three dimensional space $\mathcal{R}$ in $H^1(\Omega)$. Such a subspace can be found by the following construction: Fix a basis $\{\psi^1, \psi^2, \psi^3\}$ of $\mathcal{R}$ and three continuous linear functionals $F_j \in (H^1(\Omega))^*$ with $F_j(\psi^k) = \delta_{j,k}$, where $\delta_{j,k}$ is the KRONECKER symbol, and put

$$H_{\mathcal{R}} := \bigcap_{j=1}^{3} \ker \ker(F_j).$$

Then $Q_{\mathcal{R}} u := \sum_{j=1}^{3} F_j(u)\psi^j$ defines a continuous linear projection onto $\mathcal{R}$, while $P_{\mathcal{R}} u := u - Q_{\mathcal{R}} u$ is a continuous linear projection onto $H_{\mathcal{R}}$. Of course, $H_{\mathcal{R}}$ and $\mathcal{R}$ are not $H^1(\Omega)$-orthogonal in general. Following [BS02, p.285], we choose the basis

$$\psi^1 = \begin{pmatrix} 1 \\ 0 \end{pmatrix}, \qquad \psi^2 = \begin{pmatrix} 0 \\ 1 \end{pmatrix}, \qquad \psi^3 = x_{\mathcal{R}} - \frac{1}{|\Omega|} \int_\Omega x_{\mathcal{R}} \, dx$$

and the functionals

$$F_1(u) = \frac{1}{|\Omega|} \int_\Omega u_1 \, dx, \qquad F_2(u) = \frac{1}{|\Omega|} \int_\Omega u_2 \, dx, \qquad F_3(u) = -\frac{1}{2|\Omega|} \int_\Omega \operatorname{rot}(u) \, dx$$

with $\operatorname{rot}(u) := \partial_{x_1} u_2 - \partial_{x_2} u_1$. By this special choice, the complement of $\mathcal{R}$ in $H^1(\Omega)$ constructed above is

$$H^1_{\mathcal{R}}(\Omega) := \left\{ u \in H^1(\Omega) : \int_\Omega u \, dx = 0, \int_\Omega \operatorname{rot}(u) \, dx = 0 \right\}$$

and the Projection $P_{\mathcal{R}} : \; H^1(\Omega) \to H^1_{\mathcal{R}}(\Omega)$ is given by

$$P_{\mathcal{R}} u := u - \frac{1}{|\Omega|} \int_\Omega u \, dx + \frac{1}{2|\Omega|} \int_\Omega \operatorname{rot}(u) \, dx \left(x_{\mathcal{R}} - \frac{1}{|\Omega|} \int_\Omega x_{\mathcal{R}} \, dx \right).$$

To prove the existence of a weak solution for self-balanced right-hand sides, we use

$$|F(v)| \le c \left(\|f; L^2(\Omega)\| + \|g; H^{1/2}(\partial\Omega)\| \right) \|v; H^1(\Omega)\|.$$

Thus, F is a continuous functional on $H^1(\Omega)$. The well-known inequality of KORN's type in the following Lemma proves the coerciveness of the bilinear form $a(\cdot, \cdot)$ on $H^1_{\mathcal{R}}(\Omega)$.

Lemma 1. *For $u \in H^1_{\mathcal{R}}(\Omega)$ there exists a constant $c > 0$ with*

$$\|\varepsilon(u); L^2(\Omega)\| \ge c \|u; H^1(\Omega)\|$$

For a proof see [CC05], [KO88] or [BS02]. The existence and uniqueness of a weak solution follows now in a standard way from the LAX-MILGRAM Theorem.

Although a weak solution of the NEUMANN problem exists only for self-balanced data, the previous arguments show, that the variational problem

$$a(u, v) = (f, v)_\Omega + (g, v)_{\partial\Omega} \quad \text{for all} \quad v \in H^1_{\mathcal{R}}(\Omega) \tag{4}$$

is well-posed in $H^1_{\mathcal{R}}(\Omega)$ for any $f \in L^2(\Omega)$ and $g \in H^{1/2}(\partial\Omega)$ with $g = 0$ on Ξ. The next result shows that if f and g do not satisfy the orthogonality conditions (3), a field $u \in H^1(\Omega)$ solves a NEUMANN problem with modified right-hand sides, if u satisfies (4).

Lemma 2. *Let $u \in H^1(\Omega)$ be a solution of problem (4) with $f \in L^2(\Omega)$, $g \in H^{1/2}(\partial\Omega)$ with $g = 0$ on Ξ. Then u solves the* NEUMANN *problem (1) with right-hand sides $P^*_\Omega f$ and $P^*_{\partial\Omega} g$, where*

$$P^*_\Omega f := f - \frac{1}{|\Omega|}\left(\int_\Omega f\,dx + \int_{\partial\Omega} g\,ds\right),$$

$$P^*_{\partial\Omega} g := g - \frac{1}{2|\Omega|}\left((f, x_{\mathcal{R}})_\Omega + (g, x_{\mathcal{R}})_{\partial\Omega} - \frac{1}{|\Omega|}\int_\Omega x_{\mathcal{R}}\,dx\left(\int_\Omega f\,dx + \int_{\partial\Omega} g\,ds\right)\right) n_{\mathcal{R}}$$

PROOF: By the GAUSS Theorem, for $u \in H^1(\Omega)$ holds

$$\int_\Omega \mathrm{rot}(u)\,dx = \qquad\qquad \int_\Omega \nabla \cdot u_{\mathcal{R}}\,ds = \int_{\partial\Omega} n \cdot u_{\mathcal{R}}\,ds = -\int_{\partial\Omega} n_{\mathcal{R}} \cdot u\,ds$$

and a simple calculation proves

$$(f, P_{\mathcal{R}} v)_\Omega + (g, P_{\mathcal{R}} v)_{\partial\Omega} = (P^*_\Omega f, v)_\Omega + (P^*_{\partial\Omega} g, v)_{\partial\Omega} \qquad \text{for all} \quad v \in H^1(\Omega).$$

From $H^1(\Omega) = H^1_{\mathcal{R}}(\Omega) \oplus \mathcal{R}$ we have $a(u, v) = a(u, P_{\mathcal{R}} v)$ for all $v \in H^1(\Omega)$ and because u is a solution of problem (4) there holds

$$a(u, v) = a(u, P_{\mathcal{R}} v) = (f, P_{\mathcal{R}} v)_\Omega + (g, P_{\mathcal{R}} v)_{\partial\Omega} = (P^*_\Omega f, v)_\Omega + (P^*_{\partial\Omega} g, v)_{\partial\Omega} \tag{5}$$

for all $v \in H^1(\Omega)$. In particular we have for $v \in C^\infty_0(\Omega)$

$$(u, \mathscr{L} v)_\Omega = a(u, v) = (P^*_\Omega f, v)_\Omega,$$

which implies $\mathscr{L} u = P^*_\Omega f$ in the distributional sense. Moreover, we have $\mathscr{L} u \in L^2(\Omega)$ and the Gauss theorem in the weak formulation implies

$$a(u, v) = (\mathscr{L} u, v)_\Omega + (\mathscr{N} u, v)_{\partial\Omega}$$

for all $v \in H^1(\Omega)$. Together with (5) this leads to

$$(\mathscr{L} u - P^*_\Omega f, v)_\Omega + (\mathscr{N} u - P^*_{\partial\Omega} g, v)_{\partial\Omega} = (\mathscr{N} u - P^*_{\partial\Omega} g, v)_{\partial\Omega} = 0 \quad \text{for all} \quad v \in H^1(\Omega).$$

Since $v \in H^1(\Omega)$ is arbitrary, this implies $\mathscr{N} u = P^*_{\partial\Omega} g$. □

4. Finite Element Solutions

Consider a triangulation

$$\mathcal{T}_h = \left\{T^{(r)} : r = 1, \ldots, R_h\right\}$$

of Ω into isoparametric rectangles. In the following, we always use bilinear LAGRANGIAN finite elements and for simplicity, we assume that Ω has no reentrant corners. We also neglect curved parts of the boundary and assume

$$\bigcup_{r=1}^{R_h} \overline{T}^{(r)} = \overline{\Omega}.$$

With x^h_k, $k = 1, \ldots, N_h$ we denote the vertices of the triangulation and

$$\left\{\phi^h_i\right\}_{i=1}^N \quad \text{with} \quad \phi^h_i(x^h_k) = \delta_{i,k} \quad \text{for} \quad i, k \in \{1, \ldots, N\}$$

is a nodal basis of the space of shape functions $\mathcal{P}$. As we allow isoparametric bilinear elements $T^{(r)}$ we assume that there exist constants $h_2^{(r)} > h_1^{(r)} > 0$ and $x_0^{(r)} \in T^{(r)}$ with

$$B_{h_1^{(r)}}(x_0^{(r)}) \subset T^{(r)} \subset B_{h_2^{(r)}}(x_0^{(r)}), \qquad \frac{h_2^{(r)}}{h_1^{(r)}} < C \quad \text{for all} \quad 1 \le r \le R_h \tag{6}$$

where C does not depend on r and $B_h(x)$ is the circle with radius h around x. Moreover, we assume that every element $T^{(r)}$ is convex and we define the discretization parameter as

$$h := \max\left\{2h_2^{(r)} : 1 \le r \le R_h\right\}.$$

This conditions ensure, that the elements $T^{(r)}$ are not too degenerated and are needed for standard error estimates (see e.g. [Cia02]). To approximate vector fields, we need a vector-valued finite element space and we define a nodal basis $\{\varphi_i^h\}_{i=1,\dots,2N}$ by

$$\varphi_{2i-1}^h(x) = \phi_i^h(x)\boldsymbol{e}_1, \qquad \varphi_{2i}^h(x) = \phi_i^h(x)\boldsymbol{e}_2, \qquad i = 1,\dots,N$$

where $\boldsymbol{e}_j$ denotes the j-th unit vector. We define the finite element space

$$V_h := \left\{ v_h : v_h(x) = \sum_{i=1}^{2N} v_i \varphi_i^h(x) \right\} \subset H^1(\Omega) \cap C^0(\Omega \cup \partial\Omega)$$

and the interpolation operator

$$\Pi u : \quad H^1(\Omega) \cap C^0(\Omega \cup \partial\Omega) \longrightarrow V_h \quad \text{with} \quad \Pi u := \sum_{i=1}^{2N} u(x_i^h)\varphi_i^h(x).$$

Because the domain Ω has a crack Ξ, there is a difference between $\overline{\Omega}$ and $\Omega \cup \partial\Omega$. We cannot require, that functions are continuous over the crack and in $\overline{\Omega}$.

In the following we assume, that the data f and g are self-balanced. The Galerkin approximation problem is to find $u_h \in V_h$ with

$$a(u_h, v) = (f, v)_\Omega + (g, v)_{\partial\Omega} \quad \text{for all} \quad v \in V_h.$$

Denoting the coefficient vector of $u_h \in V_h$ by $\boldsymbol{u} := (u_1, \dots, u_{2N})^\top$, the problem is reduced to solve the system of linear equations

$$\boldsymbol{A}\boldsymbol{u} = \boldsymbol{f} + \boldsymbol{g}$$

with the stiffness matrix

$$\boldsymbol{A}_{i,j} = a(\varphi_i^h, \varphi_j^h), \qquad i,j = 1,\dots,2N$$

and the discrete right-hand side

$$(\boldsymbol{f} + \boldsymbol{g})_i = \int_\Omega f \cdot \varphi_i^h \, dx + \int_{\partial\Omega} g \cdot \varphi_i^h \, ds, \qquad i = 1,\dots,2N$$

or

$$\boldsymbol{f} + \boldsymbol{g} = \left((f_1, \phi_1^h)_\Omega + (g_1, \phi_1^h)_{\partial\Omega}, (f_2, \phi_1^h)_\Omega + (g_2, \phi_1^h)_{\partial\Omega}, \dots, (f_2, \phi_N^h)_\Omega + (g_2, \phi_N^h)_{\partial\Omega}\right)^\top.$$

Because of $\mathcal{R} \subset V_h$, there is no reason why the discrete problem should have a unique solution or is always solvable. To prove similar solvability conditions as in the continuous case, we need some more definitions. With $\boldsymbol{x} = (x_1, x_2, \dots, x_{2N})^\top := (x^h_{1,1}, x^h_{1,2}, \dots, x^h_{N,1}, x^h_{N,2})^\top$ we denote the vector of vertices and $\boldsymbol{x}_\mathcal{R} = (x_2, -x_1, \dots, x_{2N}, -x_{2N-1})^\top$ is the rotated one, similar to the continuous case. The mean value of a function $u_h \in V_h$ can be written as

$$\int_\Omega u_h \, dx = \sum_{i=1}^N \begin{pmatrix} u_{2i-1} \\ u_{2i} \end{pmatrix} (\phi_i^h, 1)_\Omega = \boldsymbol{b}_1^\top \boldsymbol{u} + \boldsymbol{b}_2^\top \boldsymbol{u}$$

and the integral over the rotation of $u_h \in V_h$ is

$$\int_\Omega \operatorname{rot}(u_h) \, dx = \int_\Omega \partial_1 u_{h,2} - \partial_2 u_{h,1} \, dx = \sum_{i=1}^N u_{2i}(\partial_1 \phi_i^h, 1)_\Omega - u_{2i-1}(\partial_2 \phi_i^h, 1)_\Omega = \boldsymbol{b}_\mathcal{R}^\top \boldsymbol{u}$$

with the vectors

$$\begin{aligned} \boldsymbol{b}_1 &:= \big((\phi_1^h, 1)_\Omega, 0, (\phi_2^h, 1)_\Omega, 0, \dots, (\phi_N^h, 1)_\Omega, 0\big)^\top \\ \boldsymbol{b}_2 &:= \big(0, (\phi_1^h, 1)_\Omega, 0, (\phi_2^h, 1)_\Omega, \dots, 0, (\phi_N^h, 1)_\Omega\big)^\top \\ \boldsymbol{b}_\mathcal{R} &:= \big(-(\partial_2 \phi_1^h, 1)_\Omega, (\partial_1 \phi_1^h, 1)_\Omega, \dots, -(\partial_2 \phi_N^h, 1)_\Omega, (\partial_1 \phi_N^h, 1)_\Omega\big)^\top. \end{aligned}$$

With the definitions $\boldsymbol{c}_1 := \big(1, 0, 1, 0, \dots, 1, 0\big)^\top$ and $\boldsymbol{c}_2 := \big(0, 1, 0, 1, \dots, 0, 1\big)^\top$, we can formulate the solvability conditions of the system of linear equations.

Lemma 3. *The linear system of equations $\boldsymbol{A}\boldsymbol{u} = \boldsymbol{f} + \boldsymbol{g}$ with $\boldsymbol{A}_{i,j} = a(\varphi_i, \varphi_j)$ and $\boldsymbol{f}_i + \boldsymbol{g}_i = (f, \varphi_i^h)_\Omega + (g, \varphi_i^h)_{\partial\Omega}$ is solvable if and only if*

$$(\boldsymbol{f} + \boldsymbol{g})^\top \boldsymbol{v} = 0 \quad \text{for all} \quad \boldsymbol{v} \in \ker(\boldsymbol{A})$$

The kernel is of the form

$$\ker(\boldsymbol{A}) = \operatorname{span}\{\boldsymbol{c}_1, \boldsymbol{c}_2, \boldsymbol{x}_\mathcal{R}\}$$

while using Lagrangian *elements. The continuous compatibility conditions*

$$(f_j, 1)_\Omega + (g_j, 1)_{\partial\Omega} = 0, \qquad (f, x_\mathcal{R})_\Omega + (g, x_\mathcal{R})_{\partial\Omega} = 0, \qquad j = 1, 2,$$

are equivalent to the discrete compatibility conditions

$$\boldsymbol{c}_1^\top (\boldsymbol{f} + \boldsymbol{g}) = 0, \qquad \boldsymbol{c}_2^\top (\boldsymbol{f} + \boldsymbol{g}) = 0, \qquad \boldsymbol{x}_\mathcal{R}^\top (\boldsymbol{f} + \boldsymbol{g}) = 0.$$

Proof: For the first conclusion, we only have to prove the representation of the kernel. Because we use Lagrangian elements, the representation

$$1 = \sum_{i=1}^N \phi_i^h(x), \qquad x_\mathcal{R} = \sum_{i=1}^N \left(x_{2i}^h \boldsymbol{e}_1 - x_{2i-1}^h \boldsymbol{e}_2\right) \phi_i^h(x)$$

is valid. For $k \in \{1, \dots, 2N\}$ it is clear that

$$0 = a(\boldsymbol{e}_j, \varphi_k^h) = \sum_{i=1}^N a(\phi_i^h \boldsymbol{e}_j, \varphi_k^h) = (\boldsymbol{A}\boldsymbol{c}_j)_k \,, \qquad j = 1, 2.$$

The same argumentation leads to $0 = a(x_{\mathcal{R}}, \varphi_k^h) = (\boldsymbol{A}\boldsymbol{x}_{\mathcal{R}})_k$. Again, by construction of the nodal basis we have

$$(f_j, 1)_\Omega + (g_j, 1)_{\partial\Omega} = \sum_{i=1}^{N} \Big((f_j, \phi_i^h)_\Omega + (g_j, \phi_i^h)_{\partial\Omega} \Big) = \boldsymbol{c}_j^\top (\boldsymbol{f} + \boldsymbol{g}), \qquad j = 1, 2$$

$$\begin{aligned}(f, x_{\mathcal{R}})_\Omega + (g, x_{\mathcal{R}})_{\partial\Omega} &= \sum_{i=1}^{N} \Big(x_{2i}((f_1, \phi_i^h)_\Omega + (g_1, \phi_i^h)_{\partial\Omega}) - x_{2i-1}((f_2, \phi_i^h)_\Omega + (g_2, \phi_i^h)_{\partial\Omega}) \Big) \\ &= \boldsymbol{x}_{\mathcal{R}}^\top (\boldsymbol{f} + \boldsymbol{g})\end{aligned}$$

The lemma is proved. □

The system of linear equations has only a solution, if the discrete right-hand side is orthogonal to the kernel of system matrix $\boldsymbol{A}$. We have proven, that this condition is fulfilled, if the data are self-balanced. Solving the linear system numerically, there is another problem. The system is not uniquely solvable and the system matrix is only semi-definite. We can not apply a standard method to solve like Conjugate Gradient. Nevertheless, such problems can be solved by the Minimal Residual method (MinRes) developed in [PS75]. But again, the computed solution is not necessarily the normalized unique one. For the continuous problem, we have solved this problems with the help of projections. It is obvious to translate this ideas to the discrete case.

The discrete projector $\boldsymbol{P}$ is given by

$$\boldsymbol{P} = \boldsymbol{I} - \frac{\boldsymbol{c}_1\boldsymbol{b}_1^\top + \boldsymbol{c}_2\boldsymbol{b}_2^\top}{|\Omega|} + \frac{1}{2|\Omega|}\left(\boldsymbol{x}_{\mathcal{R}} - \frac{\big(\boldsymbol{c}_1\boldsymbol{b}_1^\top + \boldsymbol{c}_2\boldsymbol{b}_2^\top\big)}{|\Omega|}\boldsymbol{x}_{\mathcal{R}} \right)\boldsymbol{b}_{\mathcal{R}}^\top$$

and we prove $\boldsymbol{b}_1^\top \boldsymbol{P}\boldsymbol{u} = \boldsymbol{b}_2^\top \boldsymbol{P}\boldsymbol{u} = 0$ which is equivalent to $(P_{\mathcal{R}} u_{h,j}, 1)_\Omega = 0$, $j = 1, 2$. A short calculation shows

$$\boldsymbol{b}_1^\top \frac{\boldsymbol{c}_1\boldsymbol{b}_1^\top}{(1,1)_\Omega} = \frac{1}{(1,1)_\Omega}\left(\sum_{i=0}^{N} (\phi_i^h, 1)_\Omega \right)\boldsymbol{b}_1^\top = \boldsymbol{b}_1^\top, \quad \boldsymbol{b}_2^\top \frac{\boldsymbol{c}_2\boldsymbol{b}_2^\top}{(1,1)_\Omega} = \boldsymbol{b}_2^\top, \quad \boldsymbol{b}_1^\top \boldsymbol{c}_2\boldsymbol{b}_2^\top = \boldsymbol{b}_2^\top \boldsymbol{c}_1\boldsymbol{b}_1^\top = 0$$

and we find $\boldsymbol{b}_1^\top \boldsymbol{P}\boldsymbol{u} = \boldsymbol{b}_2^\top \boldsymbol{P}\boldsymbol{u} = 0$. For our choice of finite elements it is clear that

$$1 = \sum_{i=0}^{N} \phi_i^h(x), \qquad |\Omega| = (1,1)_\Omega = \sum_{i=0}^{N} (\phi_i^h, 1)_\Omega$$

and therefore, for the derivatives of the shape functions hold

$$0 = \partial_k 1 = \sum_{i=0}^{N} \partial_k \phi_i^h(x)\Big|_{T^{(r)}}, \qquad 0 = \sum_{i=0}^{N} (\partial_k \phi_i^h, 1)_\Omega, \qquad k = 1, 2.$$

With

$$-2 = \frac{(\mathrm{rot}(x_{\mathcal{R}}), 1)_\Omega}{(1,1)_\Omega} = -\frac{1}{(1,1)_\Omega} \sum_{i=1}^{N} \Big(x_{2i-1}(\partial_1 \phi_i^h, 1)_\Omega + x_{2i}(\partial_2 \phi_i^h, 1)_\Omega \Big) = \frac{1}{(1,1)_\Omega} \boldsymbol{b}_{\mathcal{R}}^\top \boldsymbol{x}_{\mathcal{R}}$$

we get $\boldsymbol{b}_{\mathcal{R}}^\top \boldsymbol{P}\boldsymbol{u} = 0$ what means $(\mathrm{rot}(P_{\mathcal{R}} u_h), 1)_\Omega = 0$. Finally, the discrete analogue of the projector P^* is

$$\boldsymbol{P}^\top = \boldsymbol{I} - \frac{\boldsymbol{b}_1\boldsymbol{c}_1^\top + \boldsymbol{b}_2\boldsymbol{c}_2^\top}{|\Omega|} + \frac{1}{2|\Omega|}\boldsymbol{b}_{\mathcal{R}}\left(\boldsymbol{x}_{\mathcal{R}}^\top - \boldsymbol{x}_{\mathcal{R}}^\top \frac{\big(\boldsymbol{b}_1\boldsymbol{c}_1^\top + \boldsymbol{b}_2\boldsymbol{c}_2^\top\big)}{|\Omega|} \right)$$

With the same arguments one can easily proof $\boldsymbol{c}^\top \boldsymbol{P}^\top (\boldsymbol{f}+\boldsymbol{g}) = 0$ for all $\boldsymbol{c} \in \ker(\boldsymbol{A})$.

We will take great advantage of the discrete projectors in practical computations as we will see in the last paragraph. If one can compute some discrete solution $\boldsymbol{u}$, the approximation of the unique solution $u \in H^1_{\mathcal{R}}(\Omega)$ is obtained just by multiplication with $\boldsymbol{P}$. Moreover, the projector $\boldsymbol{P}^\top$ can be used to improve the precision of the discrete orthogonality conditions.

5. Numerical examples

For computations we use the C++ library deal.II developed at the Numerical Methods group at University of Heidelberg. deal.II is open source and for more information see www.dealii.org. We use structured meshes (see Figure 3) and only global refinement. We don't want to deal with local refinement or hanging nodes.

In Fracture Mechanics, one of the main interests is the computation of the stress intensity factors K_I and K_{II}. If we consider the elastic solid Ω under an external surface load $g \in H^{1/2}(\partial\Omega)$ without body forces and tension-free crack Ξ, the stress intensity factors can computed by

$$K_I = \int_{\partial\Omega} \zeta^1 \cdot g \, ds, \qquad K_{II} = \int_{\partial\Omega} \zeta^2 \cdot g \, ds$$

see e.g. [Bue70], [MP77]. The so-called weight functions ζ^j are solutions of the homogeneous problem

$$\mathscr{L}(\nabla_x)\zeta^j(x) = 0, \qquad x \in \Omega$$

$$\mathscr{N}(\nabla_x)\zeta^j(x) = 0, \qquad x \in \partial\Omega$$

with a singularity at the crack tip

$$\zeta^j(x) = r^{-1/2}\Psi^j(\vartheta) + \widetilde{\zeta}^j(x)$$

Ψ^j are smooth functions, which are known analytically for isotropic solids, see [NP96], and can be computed numerically for anisotropic ones [PB95]. Because $r^{-1/2}\Psi^j$ are solutions of the homogeneous elasticity problem in the whole plane with a semi-infinite crack, the remainder $\widetilde{\zeta}^j$ is a solution of the problem

$$\begin{aligned} \mathscr{L}(\nabla_x)\widetilde{\zeta}^j(x) &= 0, && x \in \Omega \\ \mathscr{N}(\nabla_x)\widetilde{\zeta}^j(x) &= 0, && x \in \Xi^+ \cup \Xi^- \\ \mathscr{N}(\nabla_x)\widetilde{\zeta}^j(x) &= \widetilde{p}(x), && x \in \Gamma \end{aligned} \tag{7}$$

with $\widetilde{p} := -\mathscr{N}(\nabla_x)\left(r^{-1/2}\Psi^j\right)$. Moreover, the right-hand side $\widetilde{g}$, defined by $\widetilde{g} = \widetilde{p}$ on Γ and $\widetilde{g} = 0$ on Ξ, is self-balanced and in $H^{1/2}(\partial\Omega)$. Therefore, a unique solution $\widetilde{\zeta}^j \in H^1_{\mathcal{R}}(\Omega)$ exists. For more details about weight-functions we refer to [CDD03] and [NP94, p. 278].

We take into account, that we only have to compute the solutions $\widetilde{\zeta}^j$ with finite energy by the Finite Element method. There is no need to compute solutions with singularities.

5.1 Solving the linear system

As mentioned above, we use MinRes [PS75] to solve the system $\boldsymbol{A}\boldsymbol{u} = \boldsymbol{b} := \boldsymbol{f}+\boldsymbol{g}$ with $\boldsymbol{u}_0 = \boldsymbol{0}$. MinRes is a Krylov subspace method and computes in every iteration step

$$\|\boldsymbol{b} - \boldsymbol{A}\boldsymbol{u}_k\|_2 = \min, \qquad \boldsymbol{u}_k \in \mathcal{K}_k(\boldsymbol{A}; \boldsymbol{b}), \qquad k \leq 2N \tag{8}$$

where $\mathcal{K}_k(\boldsymbol{A};\boldsymbol{b}) = \text{span}\{\boldsymbol{b}, \boldsymbol{A}\boldsymbol{b}, \ldots, \boldsymbol{A}^{k-1}\boldsymbol{b}\}$ is the Krylov subspace of dimension k. For more details about Krylov subspace methods see [Mei99] and for a detailed representation of MinRes [SVM00] also. We know, that a solution $\boldsymbol{u}$ exists, if the data are orthogonal on the kernel of $\boldsymbol{A}$. But while computing $\boldsymbol{b}$ by using quadrature formulas and in floating point arithmetic, the right-hand side is not exactly orthogonal, which is of great importance for numerical computations. MinRes computes a numerical solution, even the orthogonality conditions do not hold, but whether this is a solution of the linear system, depends on the accuracy of the orthogonality conditions. We will show this in an example.

5.2 Compact Tension specimen

We consider the classical Compact Tension (CT-) specimen subjected to two symmetric forces $F = 4500N$ in x_2-direction applied in the two holes according to Figure 2. All other faces are traction free.

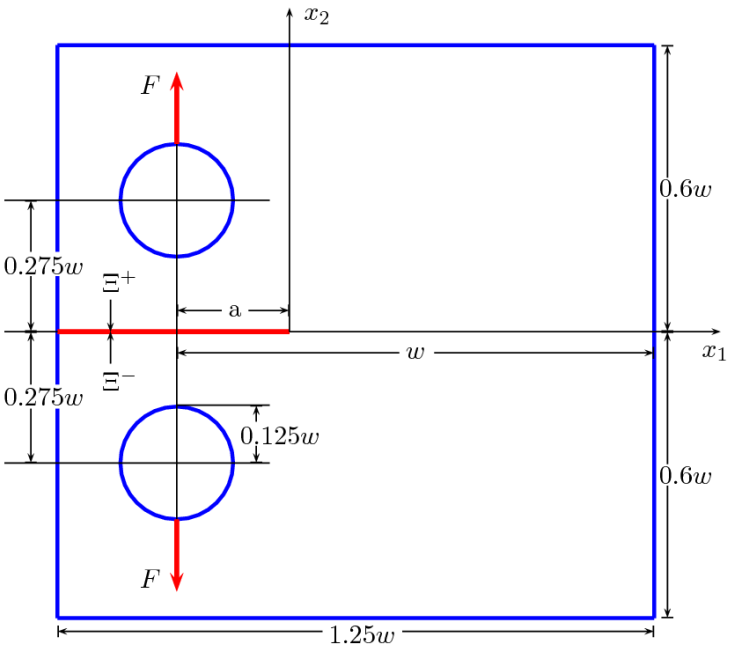

Figure 2: Compact Tension specimen

We select the length units to $w = 72mm$ and $a = 17mm$. The thickness of the specimen is $10mm$. To compare our method with well-known results, we choose the material properties

$$\lambda = 56023\ \frac{N}{mm^2} \qquad \mu = 26364\ \frac{N}{mm^2} \quad \text{or} \quad E = 70656\ \frac{N}{mm^2} \qquad \nu = 0.34$$

corresponding to aluminium alloy 7075-T651. First, we give results for the computed displacement. In [Mur87, p.18], the crack opening at the front face at point $x_0 := (-a - 0.25w, 0)$ is given by

$$\delta_0 = 0.1121\ mm \pm 0.5\%$$

and at the load line at the point $x_l := (-a, 0)$ by

$$\delta_l = 0.0586\ mm \pm 0.5\%$$

if we enforce plain strain conditions. For a symmetric loading, the displacement field of an isotropic solid is symmetric with respect to the crack. Table 4 show the computed solution and the computed projected solution at the points x_0 and x_l. The projected solution is symmetric up to 10 digits and

DoF	$\delta_{l,h}$	$\lvert\delta_l - \delta_{l,h}\rvert$	$\delta_{0,h}$	$\lvert\delta_0 - \delta_{0,h}\rvert$
198	0.0545	0.0040	0.1023	0.0098
686	0.0647	0.0061	0.1225	0.0103
2526	0.0515	0.0070	0.0982	0.0139
9662	0.0615	0.0029	0.1172	0.0051
37758	0.0577	0.0008	0.1097	0.0023
149246	0.0579	0.0006	0.1101	0.0020
593406	0.0580	0.0005	0.1103	0.0018
2366462	0.0588	0.0002	0.1114	0.0007

Table 1: Crack opening of the projected solution

Table 1 shows the resulting crack opening. Using 2366462 DoF (degrees of freedom) in the finite element computation, the relative error in the crack opening at point x_l is smaller than 0.34% and at point x_0 smaller than 0.62%.
Computing the mean value of the last solution and the integral over its rotation we have

$$\boldsymbol{b}_1^\top \boldsymbol{u} + \boldsymbol{b}_2^\top \boldsymbol{u} = -0.000393 \qquad \boldsymbol{b}_{\mathcal{R}}^\top \boldsymbol{u} = 0.000011$$

These integrals do not really vanish and the computed solution is not the normalized and unique one. In contrast, the integrals of the projected solution are

$$\boldsymbol{b}_1^\top \boldsymbol{P}\boldsymbol{u} + \boldsymbol{b}_2^\top \boldsymbol{P}\boldsymbol{u} = 4.14E-18 \qquad \boldsymbol{b}_{\mathcal{R}}^\top \boldsymbol{u} = 1.95E-19.$$

Applying the symmetric force F, the discrete orthogonality conditions are fulfilled,

$$\boldsymbol{c}_1^\top \boldsymbol{g} = 1.54E-18, \qquad \boldsymbol{c}_2^\top \boldsymbol{g} = 9.33E-19, \qquad \boldsymbol{x}_{\mathcal{R}}^\top \boldsymbol{g} = 3.98E-17$$

and there is no need to project the data to improve this results.
Next, we compute the stress intensity factors, given in [Sra76] by

$$K_I = 251.4 \, \frac{N}{mm^{3/2}} \,, \qquad K_{II} = 0. \, \frac{N}{mm^{3/2}}$$

with an accuracy of $\pm 0.5\%$ for $0.2 \leq \frac{a}{w} \leq 1.0$. Table 5 and Table 7 show the computed results without projecting the data or the solutions. As one can see, the orthogonality conditions are not fulfilled in the first iteration steps and MinRes computes no solution. To fulfill the internal stopping criterion with $eps = 1. \times 10^{-10}$, numerous iteration steps are needed, but the residual norm $\|\boldsymbol{A}\boldsymbol{u}_k - \boldsymbol{b}\|_2$ does not become small. The computed stress intensity factors are far from the exact values, not until using 37 758 DoF. Computing K_I with a finite element solution with 2 366 462 DoF, we have an error

$$|K_I - K_{I,h}| = 1.4484, \qquad \text{which means, the relative error is} \qquad \leq 0.54\%.$$

In contrast, Table 6 and Table 8 show the results while projecting the data and the solutions. The residual norm decrease linear, up to the effect of rounding errors, using more then 149 246 DoF. Computing K_I in the last iteration step, the error is

$$|K_I - K_{I,h}| = 0.2216, \qquad \text{which means, the relative error is} \qquad \leq 0.088\%.$$

This shows one advantage using discrete projections.

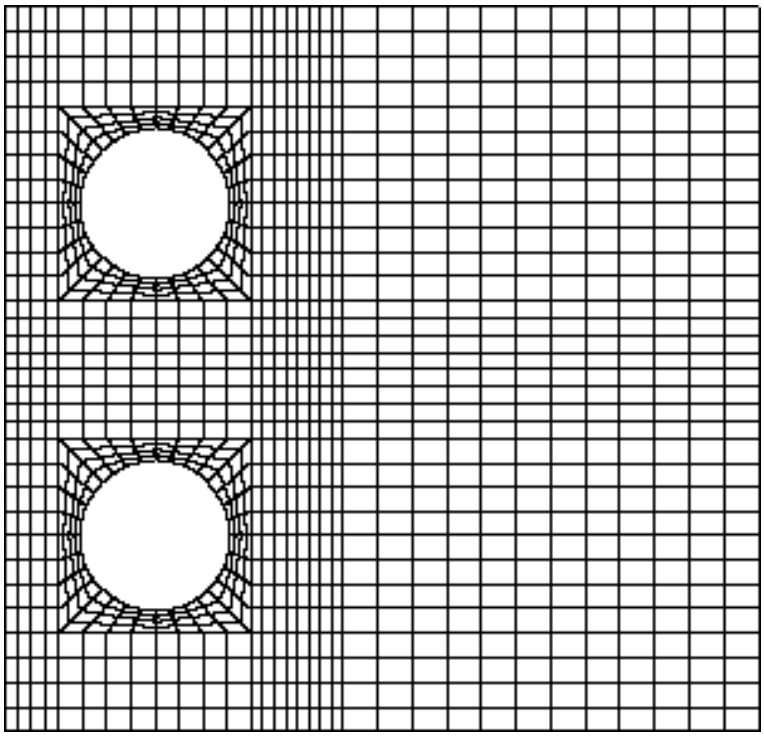

Figure 3: Used mesh with 686 DoF

In the final iteration step, the relative error of the computed values of K_I differ only by 0.45%, but the number of degrees of freedom in the finite element solution is very large and computing such a solution needs several time. Projecting the data and the solution, the relative error in K_I is less than 0.87% with only 37 758 DoF and such a finite element solution can be computed in a fractional amount of time. Without projecting, this error is about 2%. This is a real advantage of using projections and is of great interest while computing crack paths for example. Approximating the path of a crack in a solid by a polygon, one has to compute SIFs in numerous approximation steps and using projections will save a lot of computing time. We will show this in upcoming papers.

5.3 An example for an anisotropic solid

After we have shown some of the advantages and the accuracy of our projection method, we discuss an anisotropic example. We consider the CT-specimen, subjected to the same symmetric forces and again, we want to compute the stress intensity factors K_I and K_{II}. The only difference to the example before is the change of the elastic behavior of the solid. In [BSHW$^+$05, p. 2349] an orthotropic material with two planes of elastic symmetry is given. We denote this material axes by z_1 and z_2 and the angle between the material axes and the crack by β, see Figure 4. For $\beta = 0$ the material axes and the coordinate system coincide. If we change the angle β, the crack lies not in a plane of elastic symmetry and we have to rotate the elastic moduli also. Of course, this is not the case if we consider an isotropic solid. Enforcing plane stress conditions, the resulting elastic moduli for different angles β are given in Table 2.
We use the same meshes and numbers of DoF as in the isotropic example and compute the stress intensity factors K_I and K_{II} using our projection method. The results are given in Table 3. We do not present the orthogonality conditions and the numerical results without using projections for all angles and give them only for $\beta = 0$ in Table 9 and Table 10. For all other angles the difference in results look nearly the same as for $\beta = 0$.

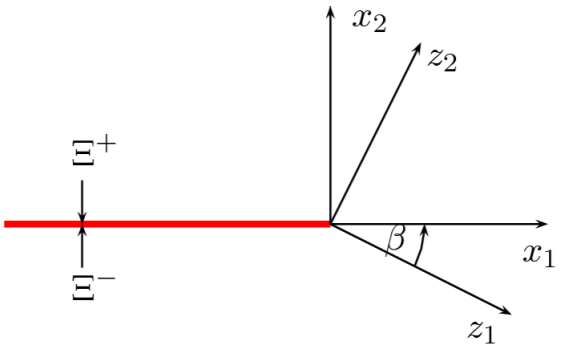

Figure 4: Material and coordinate axes

	$\beta = 0$	$\beta = 15°$	$\beta = 30°$	$\beta = 45°$
a_{11}^{11}	25128200	22038000	14711400	7344260
a_{22}^{22}	1758980	1799580	3026780	7344260
a_{22}^{11}	474924	1999760	5049430	6574260
a_{12}^{12}	385000	1909835	4959505	6484350
a_{11}^{12}	0	-5562250	-7700675	-5842314
a_{22}^{12}	0	-280065	-2418503	-5842314

Table 2: Elastic moduli for plane stress conditions

An important fact is, that the SIFs strongly depend on the angle between the axes of elastic symmetry and the crack. Even though the applied force and the solid are symmetric with respect to the crack, the stress intensity factor K_{II} is not zero and not even small compared to K_I, if $\beta \neq 0$. We can only expect that K_{II} vanishes, if the material is orthotropic and the crack lies in a plane of elastic symmetry.

We also remark, that the numerical results for K_I and K_{II} are significant worse without using our projection method as in the isotropic case. Since the results in the final steps only differ by digits while using projections, otherwise the numbers really jump and one can not see convergence.

DoF	$\beta = 0$		$\beta = 15°$		$\beta = 30°$		$\beta = 45°$	
	K_I	K_{II}	K_I	K_{II}	K_I	K_{II}	K_I	K_{II}
198	4207.25	$5.33E-08$	747.36	89.56	202.72	62.95	96.47	50.69
686	4469.93	$5.21E-08$	821.51	93.97	236.29	67.12	118.13	55.69
2526	3437.78	$4.14E-08$	643.78	66.50	190.51	49.42	98.38	42.92
9662	4053.59	$4.27E-08$	765.70	74.26	229.97	55.41	119.89	48.81
37758	3781.40	$4.11E-08$	716.95	67.41	216.96	49.97	113.74	44.25
149246	3789.58	$4.80E-08$	719.71	66.71	218.61	49.18	114.99	43.65
593406	3793.57	$5.05E-08$	721.04	66.37	219.40	48.81	115.60	43.36
2366462	3794.65	$5.45E-08$	721.64	66.45	219.79	49.01	115.94	43.52

Table 3: Computed K_I and K_{II} for different angles β

Acknowledgement: This paper is based on investigations of the collaborative research center SFB/TR

TRR 30, which is kindly supported by the DFG. The authors would like to thank Maria Specovius-Neugebauer for her helpful advices and many discussions on this work.

DoF	Iter.		$u_h(x_0)$	$P_{\mathcal{R}}u_h(x_0)$
198	54	x_0^+	$(-0.017709, +0.049081)$	$(-0.017368, +0.051172)$
		x_0^-	$(-0.017709, -0.053263)$	$(-0.017368, -0.051172)$
686	96	x_0^+	$(-0.020695, +0.060249)$	$(-0.020020, +0.061276)$
		x_0^-	$(-0.020695, -0.062303)$	$(-0.020020, -0.061276)$
2526	183	x_0^+	$(-0.016654, +0.048362)$	$(-0.015819, +0.049103)$
		x_0^-	$(-0.016654, -0.049844)$	$(-0.015819, -0.049103)$
9662	343	x_0^+	$(-0.019750, +0.057881)$	$(-0.018812, +0.058634)$
		x_0^-	$(-0.019750, -0.059387)$	$(-0.018812, -0.058634)$
37758	649	x_0^+	$(-0.018398, +0.054152)$	$(-0.017595, +0.054897)$
		x_0^-	$(-0.018398, -0.055642)$	$(-0.017595, -0.054897)$
149246	1263	x_0^+	$(-0.018394, +0.054277)$	$(-0.017649, +0.055076)$
		x_0^-	$(-0.018394, -0.055876)$	$(-0.017649, -0.055076)$
593406	2484	x_0^+	$(-0.018384, +0.054316)$	$(-0.017674, +0.055153)$
		x_0^-	$(-0.018386, -0.055998)$	$(-0.017674, -0.055153)$
2366462	4878	x_0^+	$(-0.018467, +0.054853)$	$(-0.017655, +0.055720)$
		x_0^-	$(-0.018553, -0.056587)$	$(-0.017655, -0.055720)$

Table 4: Solution and projected solution at point x_0

DoF	Iter.	$\|\boldsymbol{A}\boldsymbol{u}_k - \boldsymbol{b}\|_2$	$\boldsymbol{c}_0^\top \boldsymbol{g}_1$	$\boldsymbol{c}_1^\top \boldsymbol{g}_1$	$\boldsymbol{x}_{\mathcal{R}}^\top \boldsymbol{g}_1$	K_I
198	49780	$1.61E+15$	$4.57E-01$	$5.11E-13$	$6.36E-12$	$5.71E+10$
686	24090	$5.53E+13$	$1.97E-02$	$7.95E-13$	$1.63E-11$	$1.07E+09$
2526	163880	$1.03E+12$	$1.15E-03$	$3.19E-13$	$1.09E-11$	$4.36E+06$
9662	1662	$6.33E+09$	$7.18E-05$	$3.23E-13$	$7.73E-12$	$3.60E+04$
37758	609	$2.24E-07$	$4.48E-06$	$4.20E-13$	$5.91E-11$	247.7834
149246	1175	$5.35E-07$	$2.80E-07$	$3.14E-13$	$3.27E-11$	249.3430
593406	2297	$2.77E-06$	$1.75E-08$	$1.76E-13$	$2.09E-11$	250.1723
2366462	4459	$3.31E-05$	$1.09E-08$	$9.03E-13$	$1.90E-11$	252.8423

Table 5: Orthogonality conditions and computed K_I without projection

References

[BL05] P. Bochev and R.B. Lehoucq, *On the finite element solution of the pure Neumann problem*, SIAM Review **4** (2005), no. 1, 50–66.

[BS02] S.C. Brenner and L.R. Scott, *The mathematical theory of finite element methods*, 2nd ed., Texts in Applied Mathematics, vol. 15, Springer, Berlin, New York, 2002.

DoF	Iter.	$\|\boldsymbol{A}\boldsymbol{u}_k - \boldsymbol{b}\|_2$	$\boldsymbol{c}_0^\top \boldsymbol{P}^\top \boldsymbol{g}_1$	$\boldsymbol{c}_1^\top \boldsymbol{P}^\top \boldsymbol{g}_1$	$\boldsymbol{x}_{\mathcal{R}}^\top \boldsymbol{P}^\top \boldsymbol{g}_1$	K_I
198	56	$5.60E-02$	$2.27E-13$	$5.11E-13$	$9.09E-12$	270.7616
686	100	$1.28E-03$	$8.52E-14$	$5.68E-13$	$2.54E-11$	292.2746
2526	190	$3.87E-05$	$2.27E-13$	$3.19E-13$	$2.47E-11$	225.6401
9662	358	$1.22E-06$	$2.81E-12$	$3.23E-13$	$2.12E-10$	266.7616
37758	683	$9.52E-08$	$5.36E-12$	$3.05E-13$	$5.22E-10$	249.1829
149246	1330	$4.89E-07$	$2.59E-11$	$5.41E-13$	$8.10E-10$	249.9049
593406	2612	$2.76E-06$	$1.92E-11$	$1.76E-13$	$4.20E-10$	250.2581
2366462	5164	$1.55E-06$	$1.08E-11$	$3.17E-13$	$2.58E-10$	251.1723

Table 6: Computed Stress Intensity Factors K_I with projection

DoF	Iter.	$\|\boldsymbol{A}\boldsymbol{u}_k - \boldsymbol{b}\|_2$	$\boldsymbol{c}_0^\top \boldsymbol{g}_2$	$\boldsymbol{c}_1^\top \boldsymbol{g}_2$	$\boldsymbol{x}_{\mathcal{R}}^\top \boldsymbol{g}_2$	K_{II}
198	93103	$1.85E+15$	$8.52E-14$	$4.57E-01$	$5.70E+00$	$2.50E+11$
686	8989	$1.34E+14$	$8.52E-14$	$1.96E-02$	$1.06E-01$	$7.94E+09$
2526	13992	$9.43E+12$	$9.94E-14$	$1.15E-03$	$6.29E-02$	$2.13E+08$
9662	3805	$7.56E+10$	$1.70E-13$	$7.17E-05$	$3.89E-04$	$1.17E+05$
37758	605	$1.88E-07$	$3.26E-13$	$4.48E-06$	$2.42E-05$	$8.37E-10$
149246	1170	$2.06E-07$	$8.81E-13$	$2.80E-07$	$1.51E-06$	$1.62E-09$
593406	2282	$4.11E-07$	$5.68E-13$	$1.74E-08$	$9.47E-08$	$4.11E-09$
2366462	4390	$2.07E-06$	$4.37E-12$	$1.09E-08$	$6.12E-08$	$4.81E-08$

Table 7: Orthogonality conditions and computed K_{II} without projection

DoF	Iter.	$\|\boldsymbol{A}\boldsymbol{u}_k - \boldsymbol{b}\|_2$	$\boldsymbol{c}_0^\top \boldsymbol{P}^\top \boldsymbol{g}_2$	$\boldsymbol{c}_1^\top \boldsymbol{P}^\top \boldsymbol{g}_2$	$\boldsymbol{x}_{\mathcal{R}}^\top \boldsymbol{P}^\top \boldsymbol{g}_2$	K_{II}
198	56	$7.48E-02$	$2.84E-14$	$2.55E-13$	$1.81E-12$	$6.78E-13$
686	100	$1.33E-03$	$6.53E-13$	$7.81E-14$	$6.18E-11$	$1.55E-12$
2526	190	$4.26E-05$	$1.56E-13$	$1.42E-13$	$2.18E-11$	$1.43E-12$
9662	353	$1.47E-06$	$7.81E-14$	$2.80E-11$	$7.45E-11$	$1.47E-13$
37758	673	$5.46E-08$	$1.44E-12$	$5.10E-11$	$3.56E-10$	$4.28E-12$
149246	1312	$6.47E-08$	$3.55E-13$	$2.61E-10$	$6.18E-10$	$1.51E-11$
593406	2576	$3.65E-07$	$4.68E-13$	$1.93E-10$	$3.09E-10$	$2.19E-11$
2366462	5051	$2.02E-06$	$1.37E-12$	$1.08E-10$	$1.22E-10$	$1.10E-10$

Table 8: Orthogonality conditions and computed K_{II} with projection

DoF	Iter.	$\|\boldsymbol{A}\boldsymbol{u}_k - \boldsymbol{b}\|_2$	$\boldsymbol{c}_0^\top \boldsymbol{g}_1$	$\boldsymbol{c}_1^\top \boldsymbol{g}_1$	$\boldsymbol{x}_{\mathcal{R}}^\top \boldsymbol{g}_1$	K_I
198	34030	$4.48E+17$	98.3139	$4.83E-08$	$2.25E-06$	$-3.04E+14$
686	27483	$2.32E+15$	12.7839	$3.79E-08$	$2.17E-06$	$1.78E+12$
2526	97671	$4.48E+13$	1.8272	$2.93E-08$	$2.01E-06$	$-7.72E+09$
9662	12394	$1.00E+12$	$4.23E-02$	$2.50E-08$	$1.90E-06$	$1.61E+07$
37758	1502	$3.01E+00$	$2.54E-03$	$2.48E-08$	$1.01E-06$	3771.11
149246	1573	$1.03E-04$	$5.82E-04$	$2.31E-08$	$9.57E-07$	3787.73
593406	2899	$6.37E-05$	$4.19E-05$	$1.86E-08$	$8.98E-07$	3799.78
2366462	5682	$3.87E-04$	$3.89E-05$	$1.91E-08$	$9.93E-07$	3832.05

Table 9: Orthogonality conditions and computed K_I without projection for the orthotropic material ($\beta = 0$)

DoF	Iter.	$\|\boldsymbol{A}\boldsymbol{u}_k - \boldsymbol{b}\|_2$	$\boldsymbol{c}_0^\top \boldsymbol{g}_2$	$\boldsymbol{c}_1^\top \boldsymbol{g}_2$	$\boldsymbol{x}_{\mathcal{R}}^\top \boldsymbol{g}_2$	K_{II}
198	407692	$9.09E+16$	$2.29E-07$	$2.59E+01$	$6.34E+01$	$1.10E+13$
686	23472	$3.38E+14$	$2.02E-07$	$1.04E+00$	$1.23E+01$	$-1.44E+11$
2526	83432	$7.62E+13$	$1.79E-07$	$4.48E-01$	$1.88E+00$	$2.78E+09$
9662	2407	$5.37E+12$	$1.29E-07$	$8.90E-03$	$9.84E-01$	$-5.85E+07$
37758	2170	$1.17E+11$	$1.26E-07$	$1.93E-03$	$1.47E-01$	$1.07E+06$
149246	2097	$3.85E-01$	$9.18E-08$	$6.17E-04$	$8.74E-03$	$4.34E-01$
593406	3678	$4.34E-03$	$1.68E-08$	$7.35E-05$	$6.83E-04$	$5.38E-03$
2366462	6472	$1.02E-06$	$5.52E-08$	$9.21E-06$	$3.72E-06$	$7.99E-08$

Table 10: Orthogonality conditions and computed K_{II} without projection for the orthotropic material ($\beta = 0$)

[BSHW+05] L. Banks-Sills, I. Hershkovitz, P.A. Wawrzynek, R. Eliasi, and A.R. Ingraffea, *Methods for calculating stress intensity factors in anisotropic materials: Part I*, Eng. Frac. Mech. **72** (2005), 2328–2358.

[Bue70] H.F. Bueckner, *A novel principle for the computation of stress intensity factors*, ZAMM Z. Angew. Math. Mech. **50** (1970), 529–546.

[CC05] P.G. Ciarlet and C. Ciarlet, *Another approach to linearized elasticity and a new proof of Korn's inequality*, Math. Mod. Meth. Appl. Sci. **15** (2005), no. 2, 259–271.

[CDD03] M. Costabel, M. Dauge, and R. Duduchava, *Asymptotics without logarithmic terms for crack problems*, Commun. Partial Differ. Equations **28** (2003), no. 5-6, 869–926.

[Cia02] P.G. Ciarlet, *The finite element method for elliptic problems*, Classics in Applied Mathematics, vol. 40, SIAM, Philadelphia, 2002.

[KO88] V.A. Kondratiev and O.A. Oleinik, *Boundary-value problems for the system of elasticity theory in unbounded domains. Korn's inequalities*, Russian. Math. Surveys **43** (1988), no. 5, 65–119.

[Mei99] A. Meister, *Numerik linearer Gleichungssysteme*, Vieweg-Verlag, Braunschweig, 1999.

[MP77] V.G. Maz'ya and B.A. Plamenevsky, *The coefficients in the asymptotic forms of the solutions of elliptic boundary-value problems in domains with conical points*, Math. Nachr. **76** (1977), 29–60.

[Mur87] Y. Murakami, *Stress intensity factors handbook*, vol. 1, Pergamon Press, Oxford, New York, 1987.

[NP94] S.A. Nazarov and B.A. Plamenevsky, *Elliptic problems in domains with piecewise smooth boundaries*, de Gruyter Expositions in Mathematics, vol. 13, Walter de Gruyter and Co, Berlin, New York, 1994.

[NP96] S.A. Nazarov and O.R. Polyakova, *Rupture criteria, asymptotic conditions at crack tips, and self-adjoint extensions of the Lamé operator*, Trudy Mosk. Mat. Obshchestva **57** (1996), 16–74.

[PB95] P.J. Papadakis and I.A. Babuska, *A numerical procedure for the determination of certain quantities related to the stress intensity factors in two-dimensional elasticity*, Comput. Methods Appl. Mech. Engrg. **122** (1995), 69–92.

[PS75] C.C. Paige and M.A. Saunder, *Solution of sparse indefinite systems of linear equations*, SIAM J. Numer. Anal. **12** (1975), 617–629.

[Sra76] J.E. Srawley, *Wide range stress intensity factor expressions for ASTM E399 standard fracture toughness specimens*, Int. J. Frac. Mech. **12** (1976), 475–476.

[SVM00] G.L.G. Sleijpen, H.A. van der Vorst, and J. Modersitzki, *Differences in the effects of rounding errors in Krylov solvers for symmetric indefinite linear systems*, SIAM J. Matrix Anal. Appl. **22** (2000), no. 3, 726–751.